Title Page

Author names and affiliations: Nabodita Sinha[a], Avinash Y. Gahane[aΘ], Talat Zahra[aΘ], Ashwani K. Thakur[a*]

[a]Department of Biological Sciences and Bioengineering, Indian Institute of Technology Kanpur, UP-208016, India.

***Corresponding author:** Prof. A.K.Thakur (akthakur@iitk.ac.in)

[Θ] Equal contribution by authors

Title: Protein reservoirs of seeds are composites of amyloid and amyloid-like structures

Abstract

The functional roles of amyloids are known across diverse species, but their natural presence in plants remains underexplored. We show that monocot and dicot seed storage proteins, owing to their aggregated state, similar to protein-bodies of other species, are amyloidic. By using gold-standard amyloid probes, we reveal that the seed storage proteins exhibit a speckled pattern of amyloids interspersed in an amyloid-like matrix, suggesting their composite nature. Moreover, these structures degrade in a stepwise manner during germination and are sensitive to gibberellic acid.

The study of seed storage proteins in monocots can be traced back to 1745, when the isolation of wheat gluten was first described.(1) Analysis of dicot seed storage proteins initiated a century later with crystallization of Brazil nut globulins.(2) The discoveries were followed by detailed biochemical studies based on the extraction and solubility properties of the storage proteins.(1) The monocot seeds consist of the peripheral layers of aleurone and sub-aleurone cells, which have both storage and secretory functions.(3, 4) The endosperm cells on the other hand are exclusively for storage and are packed with starch and protein bodies.(5) In dicots, on the contrary, the cotyledon cells occupy the maximum volume of the seeds and are the sole reservoir cells.

The protein storage bodies of aleurone cells are mainly comprised of storage proteins such as 7S globulins. Proteomic analysis also suggests the presence of sequestered enzymes, heat shock proteins and defense peptides in these structures.(6) In addition, these protein bodies also contain inorganic mineral-rich globoids and lipid bodies.(7, 8) In dicot seeds, the cotyledon cells are more or less uniform and contain starch granules embedded in a protein matrix.(9, 10) This protein matrix comprises of storage protein bodies and are mainly composed of aggregates of globulins including vicilin and legumin.(11, 12) Most of these storage proteins are targeted in association with the Golgi body, leading to the formation of aggregated electron-rich protein bodies.(1, 13, 14)

The protein bodies are not unique to plant seeds. Similar structures of electron-rich dense aggregates of proteins are found in diverse species, ranging from inclusion bodies of bacteria to Russell bodies of humans.(15) Interestingly, some of them also act as storage reservoirs.

For example, metabolic enzymes assemble into aggregates in order to protect the proteins from stress in yeast,(16) while proteasome storage granules sequester and store the proteasomes for safe-keeping and recycling.(17) Sup35 in yeast still retains function in their aggregated state and acts as a translation release factor.(18)

Protein aggregates in general, can acquire multiple polymorphic structures. These include native reversible aggregates, partially unfolded globular protein aggregates, aggregate precursors (oligomers or protofibrils) and fibrillar aggregates including amyloids.(19, 20) The ultrastructural and biological properties of these aggregates depend on their type and pathway of formation. Although there has been reports suggesting disulfide bond formation, roles of molecular chaperones and specific protein-protein interaction resulting in the formation of the protein aggregates as seed storage structures,(7) little is known about the biophysical aspects of these structures in terms of type of physical interactions, or aggregate types leading to amyloid formation tendencies. Considering the fact that the protein bodies of bacteria, yeast and even humans are often associated with amyloid or amyloid-like fibrils with high stability and similar functions of storage, we hypothesize that the plant seed protein bodies owing to their aggregation might possess amyloid or amyloid-like characteristics for performing functional roles.

To detect amyloids in plants, previous reports used heterologous systems of expression and experimental conditions to induce protein aggregation.(21) But these systems do not essentially reflect the inherent amyloid nature of the plant proteins *in-vivo*. In a recent study on vicilin, this protein is shown to be amyloidogenic by computational analysis, Thioflavin T (ThT) staining of seed section and *in-vitro* aggregation.(22) However, ThT alone is not enough to confirm amyloid presence and needs to be validated using orthogonal probes. Moreover, the results obtained *in-vitro*, might not reflect the true behavior of these proteins in physiological context.

The functional aspects of endogenous amyloids in plant physiological processes such as germination, is also lacking. Germination takes place in distinct phases in both monocots and dicots. In both types of seeds, previous studies have suggested that the overall protein content remains same without any significant day-to-day changes till seedlings emerge. Although the storage protein reserves are degraded with germination time, there is an upregulation of the enzymes, keeping the overall protein percentage at par.(23, 24) However, although the total protein content remains unchanged throughout germination, the fraction of soluble protein

content increases significantly during the germination stages in multiple species.(25, 26) Nonetheless, it is not known whether the amount of the soluble protein is contributed by the degradation of any amyloidic structures. It is also important to ascertain the differential roles of amyloids and amyloid-like aggregates during degradation. Moreover, since plant hormones such as gibberellic and abscissic acid play a major role in the degradation of seed protein bodies, their effect on the amyloidic aggregates also remains to be seen. For this purpose, seed protoplasts can be an ideal choice since these are free of cell walls and other structures which might lead to staining hindrance in tissues.

In order to detect amyloids on seed sections, we used two molecular rotors ThT and Proteostat®, which are popularly used for detection of amyloid or amyloid-like protein aggregates. Although ThT is popular for understanding aggregation kinetics, detection and quantification studies, it must be validated using novel probes with enhanced properties suited for biological samples. Proteostat® is a recently discovered molecular rotor and has higher specificity and sensitivity compared to ThT,(27) and this fluorogenic probe was further used to confirm ThT dataset. Moreover, to comply with the International Society of Amyloidosis (ISA) guidelines for amyloid detection in tissue sections and biological samples, Congo red staining was performed which is till date the 'gold standard' test for amyloids.(28) In this study, we have shown that the monocot seeds of wheat (*Triticum aestivum*), and barley (*Hordeum vulgare*) and dicot seeds of chickpea (*Cicer arietinum*) and mungbean (*Vigna radiata*) show intense amyloidic signatures in the protein storage bodies of the aleurone and cotyledon cells and the amyloid-like but not the amyloid signals lose their intensity during seed germination, reflecting on the differential roles of these two structures in nutrient mobilization.

Before using amyloid-specific probes to detect amyloid presence in seed storage proteins, the sections were dual-stained with acid fuchsin and calcofluor white to demarcate the proteinaceous and cellulose-rich regions.(29, 30) As shown in **Figure 1**, seed coat, aleurone layer, and endosperm cytoplasm of monocot **(Figure 1 a-c)** and cotyledon cell-matrix of dicot seed sections **(Figure 1 d-f)** are stained with acid fuchsin and exhibit a pinkish-magenta colour on binding with proteins. Calcofluor white staining leads to a blue-fluorescence in the cell wall regions of monocots **(Figure 1c)** and dicots **(Figure 1f),** and represent cellulose-rich regions**.** To further confirm the integrity and structural aspects of the seed sections, scanning electron microscopy (SEM) was performed on wheat and mungbean seed sections. In **Figure 1g,** the dense granular cytoplasm representing protein bodies of the intact aleurone cells of

wheat is visible. Mungbean cotyledon cells, on the other hand in **Figure 1h** shows starch granules visible on the protein storage matrix.

To demarcate amyloid or amyloid-like deposits in the seed storage structures, we chose Thioflavin-T (ThT) as the first probe. It is one of the most popular dyes for amyloid or amyloid-like deposit detection and studying *in-vitro* aggregation kinetics.(31, 32) ThT dataset was validated by another molecular rotor, Proteostat®. It is a recently discovered probe, designed to detect intracellular and extracellular amyloids or amyloid-like deposits even if the amyloidogenic proteins are sparse.(33-35) For detecting amyloids or amyloid-like aggregates in seeds, wheat **(Figure 1i and 1j),** barley **(Figure 1k and 1l),** chickpea **(Figure 1m and 1n)** and mungbean **(Figure 1o and 1p)** seed sections were stained with ThT and visualized using a confocal microscope. In the monocot seeds, intense fluorescence intensity was observed in the aleurone layer compared to the endosperm. The intensity of protein storage bodies of aleurone, sub-aleurone, and endosperm cells of the seed sections was quantified to confirm this. The aleurone layer intensity of wheat **(Figure 1q)** and barley **(Figure 1r)** was significantly higher than the sub-aleurone layer and endosperm. In the dicot seed sections, matrix protein storage bodies produce an intense green fluorescence. The data obtained from both monocots and dicots suggest the amyloidic behavior of the protein storage bodies. In Proteostat® stained sections, the images show comparable pattern similar to micrographs of ThT stained seed sections, of barley **(Figure 1s)**, and chickpea **(Figure 1t)**, confirming the presence of amyloid or amyloid-like structures in seed storage bodies.

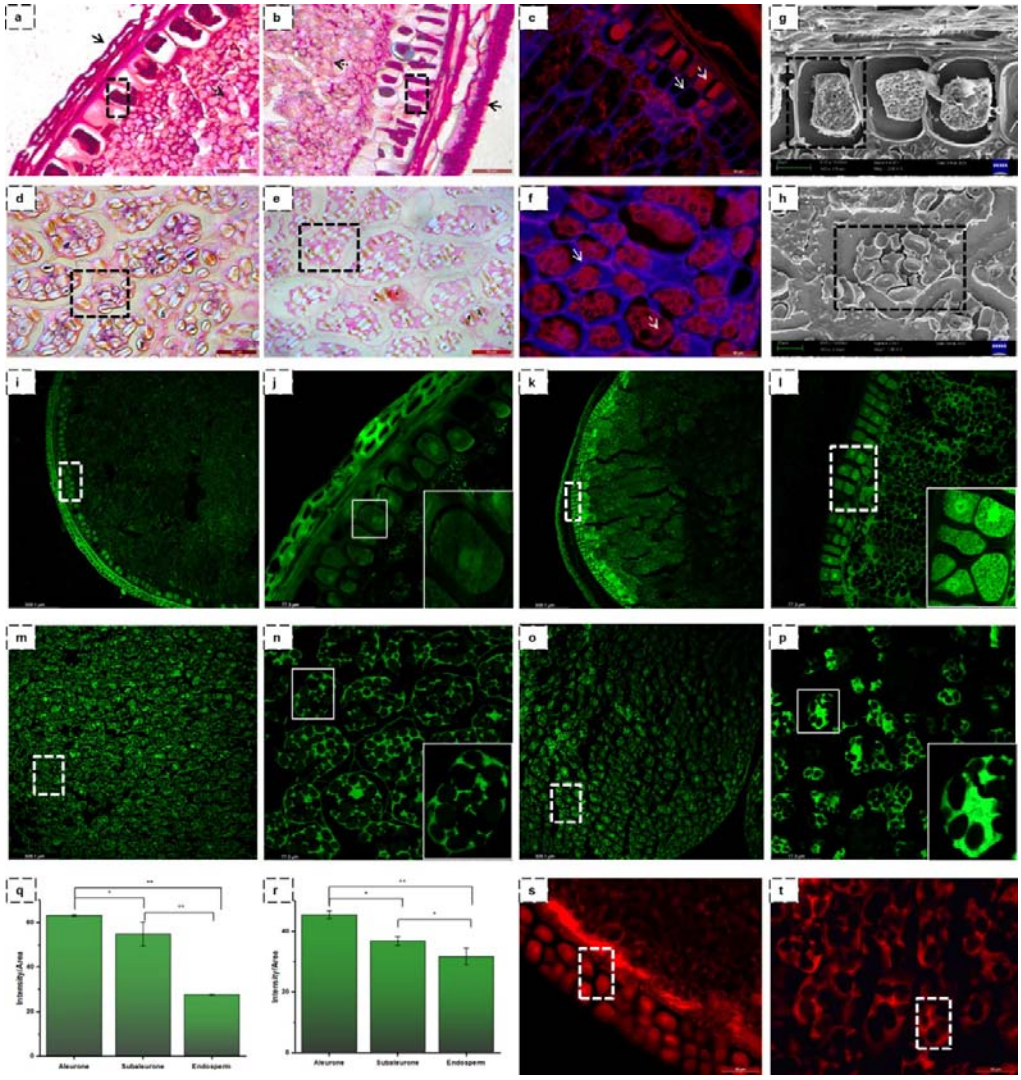

Figure 1 Analysis of amyloid-like aggregates in proteinaceous regions of seed sections. The protein-specific dye, acid fuchsin, exhibits characteristic magenta color in the seed coat (solid black arrow), aleurone (black dashed boxes), and sub-aleurone layer (black dashed arrow) of wheat (*Triticum aestivum*) (a) and barley (*Hordeum vulgare*) (b). In the dicot seeds, the stain is visible in the protein storage bodies of cotyledon cells (black dashed boxes) of chickpea (*Cicer arietinum*) (d) and mungbean (*Vigna radiata*) (e). Acid fuchsin stains the aleurone and cotyledon cells prominently, exhibiting the proteinaceous deposits in these cells. In dual staining of acid fuchsin and calcofluor white, the wheat aleurone cells (c) and mungbean cotyledon cells (f) exhibit red fluorescence in proteinaceous regions, whereas calcofluor white produces blue fluorescence in cell wall regions. Solid white arrows represent cell walls, whereas dashed white arrows represent the protein storage bodies. SEM (Scanning Electron Microscopy) analysis of wheat (g) and mungbean (h) reveal that the structure of the aleurone and cotyledon cells is maintained after histological processing. (Gamma value for each bright-field image ranges from 0.6-0.9, the changes in brightness/contrast has been applied to the whole image) ThT staining of monocot seeds reveals that both wheat (i, j and q) and barley (k, l and r) exhibit an intense fluorescence in the aleurone layer compared to the endosperm cells, suggesting an enrichment of amyloid-like protein aggregates in these regions. The dicot seeds of chickpea (m and n) and mungbean (o and p) exhibit an intense signal in the protein storage bodies of cotyledons. The white dashed boxes represent intense fluorescing areas of 10X magnified images and white solid lined boxes represent similar areas in 40X magnified images. The insets represent magnified portions of the solid-lined boxes. (Student's t-test; barley: *p=0.02, **p=0.003; wheat: *p=0.01, **p=0.003) The bar graphs represent each type of tissue's intensity/area ratio, i.e., for aleurone, subaleurone and endosperm. The ratio of five z-stacks are averaged for this purpose and

plotted as bar graphs with error bars representing standard error of the mean. (Gamma and intensity value for each confocal image is kept same for quantification purposes) Proteostat staining exhibits that the monocot seeds of barley (s) and dicot seeds of chickpea (t) demonstrate the presence of possible amyloids or amyloid-like aggregates in the protein storage bodies of aleurone and cotyledon cells as evident from the red fluorescence in these areas. White dashed boxes represent the intense signal in a representative area. (Gamma values for each image ranges from 0.8-2.5 to bring uniformity, changes in brightness/contrast has been applied to the whole image) Each experiment involves the analysis of at least three sections of at least three seeds of each type. (Scale bars for wide-field microscopy are presented on lower right corner whereas for confocal is at lower left corner)

To confirm the presence of amyloid deposits in the storage bodies of aleurone and the cotyledon cells, seed sections were stained with Congo red (CR) and the samples were visualized between two polarizers.(28, 36) A characteristic apple-green birefringence of amyloids was observed in the aleurone protein storage bodies of wheat **(Figure 2 a-d)** and barley **(Figure 2 e-h) (Supplemental Movie 1 and 2).** Fascinatingly, unlike ThT and Proteostat® staining, which showed intense signal in the whole proteinaceous region of the aleurone cells, CR-induced birefringence was observed in some of these regions. Similar case was observed for the cotyledon cells of chickpea **(Figure 2 i-l)** and mungbean **(Figure 2 m-p) (Supplemental Movie 3 and 4)**. The simultaneous presence of CR-stained amyloids interspersed between amyloid-like structures suggests a composite structure of seed storage proteins.

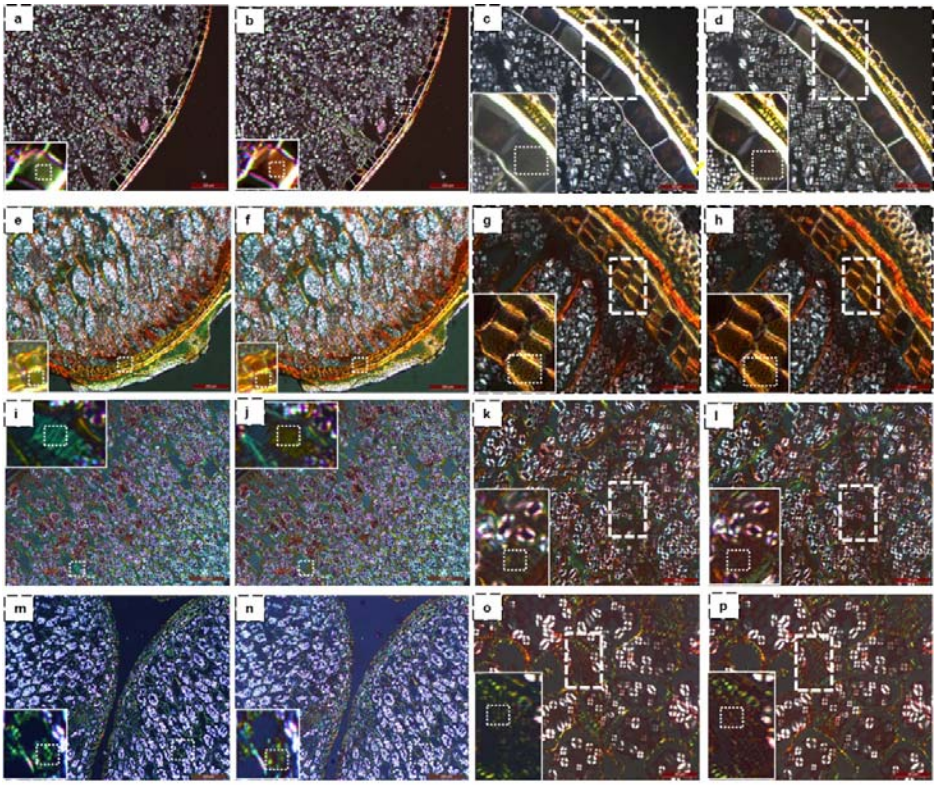

Figure 2 Confirmation of amyloids in seed sections by CR staining and functional implications of amyloids. Left two panels represent the apple-green to red birefringence when the sample is placed between two polarisers at 10X magnification. The right two panels show the same at 40X magnification. Both wheat (*Triticum aestivum*) (a-d) and barley (*Hordeum vulgare*) (e-h) aleurone cells show a visible change in the apple-green birefringence, characteristic of amyloids as indicated by the white dashed boxes inside the insets**.** Similar changes in birefringence are observed in some regions of the protein storage bodies of cotyledon cells of chickpea (i-l) (*Cicer arietinum*) and mungbean (*Vigna radiata*) (m-p). (Gamma values for 10X panels vary from 0.6-1.21, while for 40X panel, Gamma ranges from 0.5-0.9 for facilitating clear birefringence visualization, no changes in imaging parameters were done while rotating polarizer; the insets have been enhanced regarding brightness/contrast for clear presentation)

To establish the role of amyloidic aggregates in seed germination, and to ascertain the possible differential stability or degradation properties of amyloids and amyloid-like structures, the monocot and dicot seeds were allowed to germinate by imbibing water. At different time-intervals, the seeds were fixed, sectioned and stained with CR and ThT to detect the changes in the amyloids and amyloid-like structures respectively. The wheat seeds were stained at 4 **(Figure 3 a,b),** 8 **(Figure 3 c,d),** 24 **(Figure 3 e,f),** 48 **(Figure 3 g,h),** 72 **(Figure 3 i,j)** and 96 **(Figure 3 k,l)** hours, whereas the dicot seeds were stained at 8 **(Figure 3 m,n),** 24 **(Figure 3 o,p),** 48 **(Figure 3 q,r)** and 72 **(Figure 3 s,t)** hours. In the monocot seed sections, the amyloid structures were present till 48 hours, but were not detectable at 72 and 96 hours in the aleurone cells, suggesting a possible degradation of these structures. In the dicot seed sections, the amyloids were detected till 72 hours, suggesting that upto these time-point, amyloids are not degraded to the full extent. For dicot seeds, tissue processing was not possible beyond 48 hours due to fragile nature of the seeds.

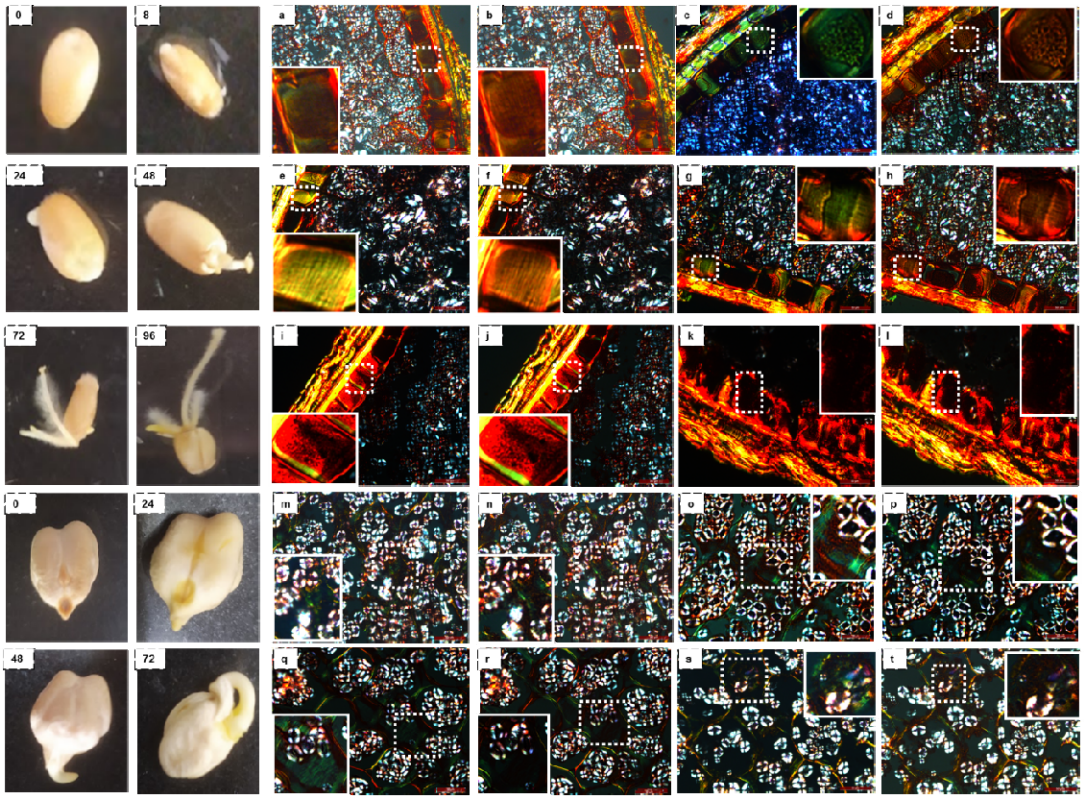

Fig 3: Congo red staining of germinated seeds to detect changes in amyloid level. The left two panels represent the seed images at different time points as labelled in the top-left corner. Congo red stained sections of wheat are represented for germination at 4 (Figure 3 a,b), 8 (Figure 3 c,d), 24 (Figure 3 e,f), 48 (Figure 3 g,h), 72 (Figure 3 i,j) and 96 (Figure 3 k,l) hours, whereas the dicot seeds were stained at 8 (Figure 3 m,n), 24 (Figure 3 o,p), 48 (Figure 3 q,r) and 72 (Figure 3 s,t) hours. In case of monocots, the amyloids are evident till 48 hours whereas in dicots, the amyloids are detected throughout all the time-points.

In order to detect the changes in the presence of amyloid-like structures, the seed sections were stained with ThT after allowing germination upto the same time periods. Also the ThT fluorescence of the seed sections are compared to the Congo red fluorescence of the seed sections at the same time-points to detect the changes in amyloid-like vs amyloid structures. **Figure 4 a-f** represents ThT staining of wheat seeds at 4, 8, 24, 48, 72 and 96 hours respectively and show a decrease in fluorescence intensity apparent from 4 hours in the aleurone cells. The CR fluorescence however decreases from 72 hours onwards **(k-p)**. In the dicot seed sections **(g-j),** the ThT fluorescence of the cotyledon matrix also shows a similar decrease in intensity from 24 hours, whereas the CR fluorescence remains similar till 72 hours **(q-t).** Collectively, the CR-birefringence **(Figure 3)** and ThT-CR fluorescence dataset **(Figure 4)** reflects on the possibility of a slower degradation of amyloid structures as compared to amyloid-like aggregates.

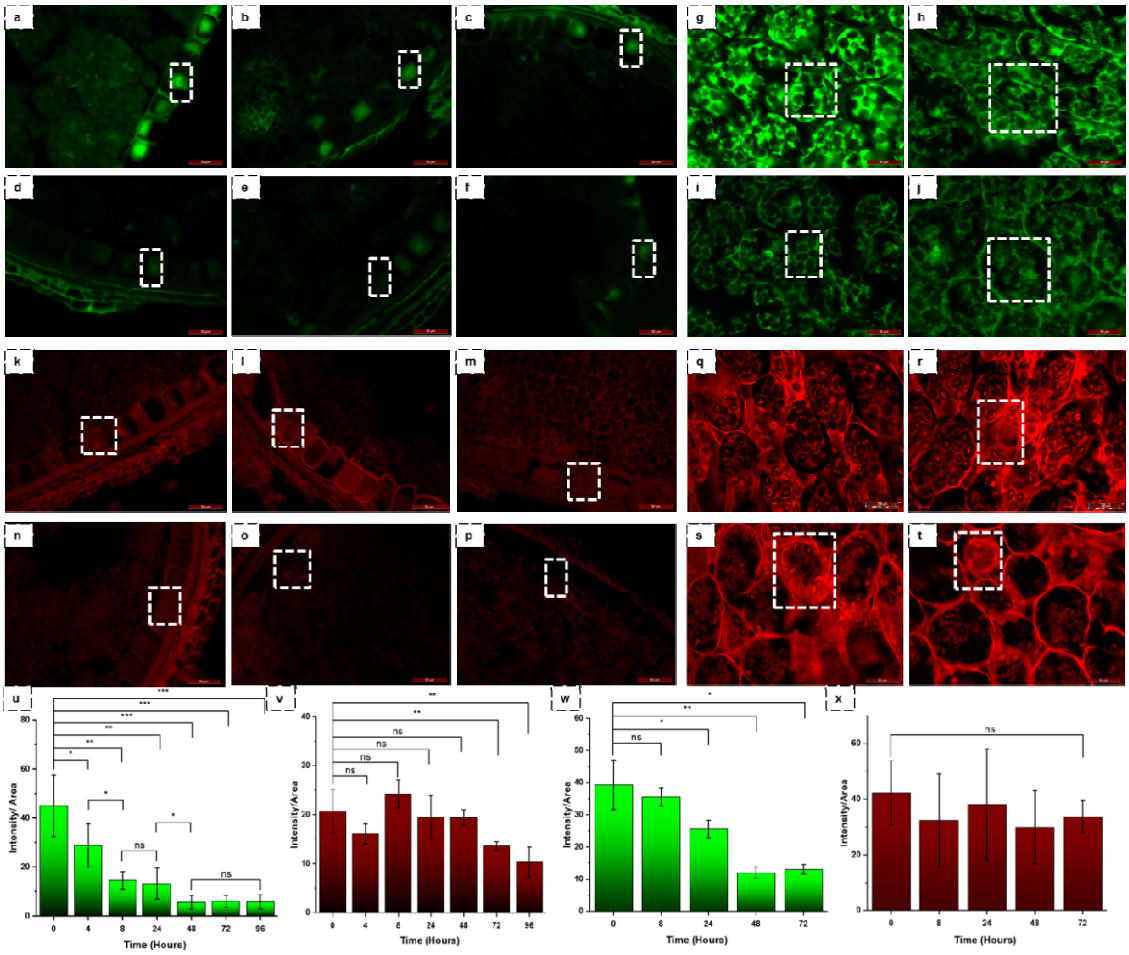

Figure 4: ThT and CR fluorescence of germinated seeds to detect amyloids vs amyloid-like aggregates. ThT staining of wheat seeds are represented at 4 (a), 8 (b), 24 (c), 48 (d), 72 (e) and 96 (f) hours. CR staining of wheat seeds are represented at 4 (k), 8 (l), 24 (m), 48 (n), 72 (o) and 96 (p) hours. ThT staining of chickpea seeds are represented as 8 (g), 24 (h), 48 (i) and 72 (j), and CR staining of chickpea seeds are represented as 8 (q), 24 (r), 48 (s) and 72 (t), Quantification of the signals are represented at ThT of wheat (u), CR of wheat (v), ThT of chickpea (w) and CR of chickpea (x). ThT signal in monocots start decreasing since 4 hours and in dicots from 24 hours. The CR fluorescence however decreases after 72 hours in monoocts and does not decrease significantly till 72 hours in dicots.

Germination in seeds is regulated by several plant hormones such as gibberellic and abscisic acid. Therefore, we hypothesized that these hormones might have a role in the degradation of the amyloidic aggregates. Since these biochemical properties cannot be followed in fixed seeds, we isolated protoplasts of monocot aleurone cells and cotyledon cells of dicots. The protoplasts were then treated with gibberellin, abscisic acid and a mixture of both and the protoplasts were stained with ThT and imaged immediately and after 8 hours. Figure **5 (a-d)** and **(g-j)** represents the barley aleurone and chickpea cotyledon protoplasts treated with incubation buffer, gibberellic, abscisic and gibberellic with abscissic acid respectively at 0

hour. **Figure 5 (e-h)** and **(k-n)** represents the prototoplasts after 8 hours. The gibberellic acid treated protoplasts show a decrease in ThT fluorescence **(f and l)** for both monocots and dicots. The abscisic acid treated protoplasts show a similar intensity **(g and m)** compared to control, whereas treatment with the mixture decreases the intensity in monocots but disrupts the shape in dicots.

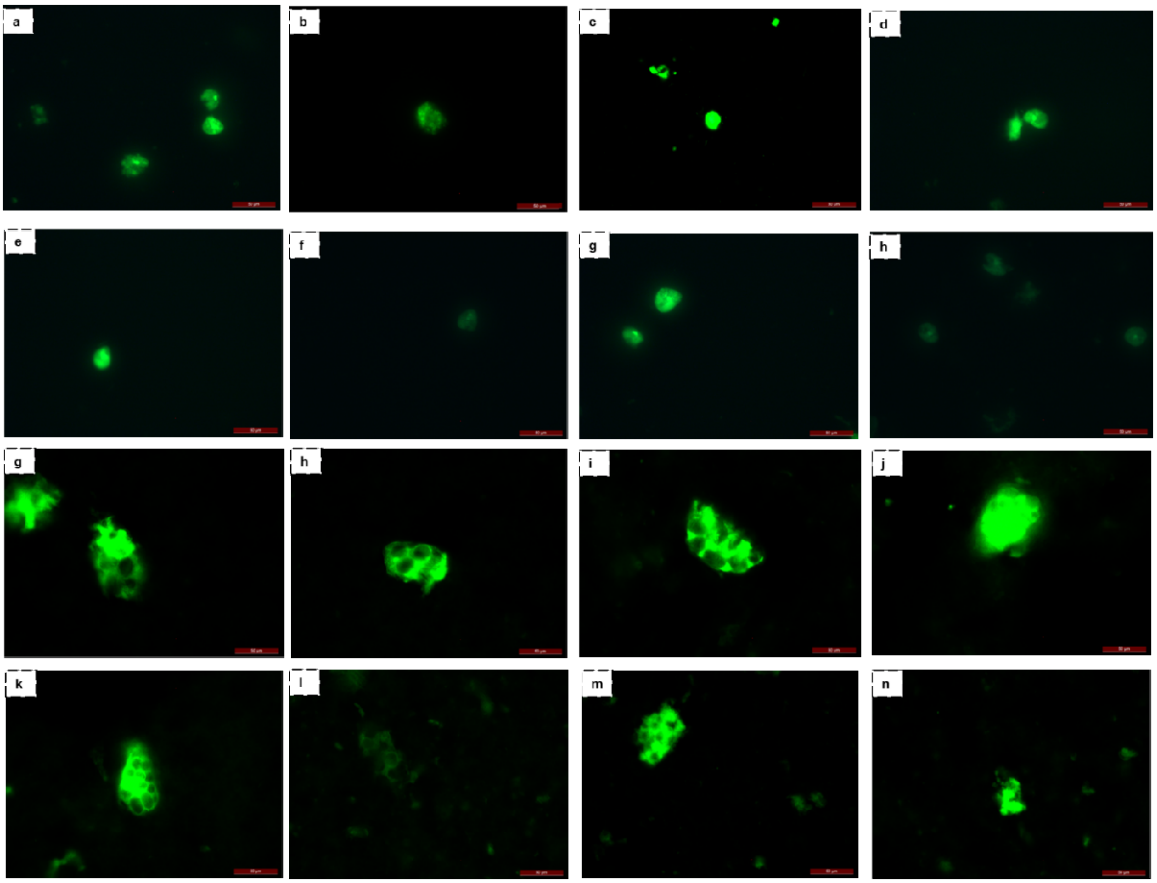

Figure 5: Effect of plant hormones on amyloidic aggregates. (a-d) represents 0-hour barley aleurone protoplasts treated with buffer, gibberellin, abscisic acid and gibberellic+abscisic acid. (e-h) represents similar treatments after 8 hours. (g-j) represents 0-hour chickpea cotyledon protoplasts treated with buffer, gibberellin, abscisic acid and gibberellic+abscisic acid, whereas (k-n) represents similar treatment counterparts after 8 hours. Gibberellin treatment decreases the amyloidic signal whereas abscisic acid maintains the fluorescence. A combined treatment of these hormones, show disruptive effects in terms of decrease in fluorescence or change in protoplast shape.

Amyloids are considered as paradoxical because of their pathogenic as well as functional roles across diverse species.(37, 38) Despite of plausible presence of amyloids in plants, the number of reports till date remains limited.(22) Although, some plant proteins have been shown to form amyloids in heterologous expression systems,(21) they do not necessarily reflect the endogenous protein behaviour. Moreover, no study has employed a combinatorial

approach with latest probes such as Proteostat® and the standard CR assay for amyloid detection. Importantly, experimental validation using multiple amyloid-specific dyes is imperative to assign amyloid or amyloid-like properties to proteins.(39)

Since the seed protein bodies are similar to other organisms' amyloidic protein bodies in morphology and functional aspects,(16) we hypothesized that the protein storage bodies of monocot and dicot seeds might contain amyloid deposits. Fascinatingly, whereas ThT and Proteostat® bound to the entire proteinaceous regions of aleurone and cotyledon cells, the birefringent signals of amyloid due to CR staining appeared in only some areas among these. Thus we conclude that the storage protein bodies of aleurone layer and cotyledon cells are comprised of amyloid and amyloid-like composite deposits. The composite structures might provide a differential role during germination where the more stable amyloid structures provide a slower release mechanism as compared to the amyloid-like aggregates. Moreover, the degradation of the amyloidic structures in presence of gibberallic and maintenance in presence of abscisic acid links the degradation in germination to the biochemical pathways, suggesting a plausible mechanism for amyloid degradation.

Amyloid presence in seed protein bodies has manifold implications in storing proteins in a structured fashion and may provide a sustained release model of nutrients during germination for embryo growth. Since amyloid formation follows pathways of nucleation and elongation,(40) the same phenomenon may explain the biogenesis of the protein bodies, as aggregated structures by self-seeding and cross-seeding of other protein components. The presence of these structures might facilitate protection of seeds from various environmental stresses.(41) The current study would open up a new avenue of research to study the protein body biogenesis and utilization at the atomic and molecular level and may illuminate the enigmatic issue of the role of functional amyloids in evolution across species.(42)

Methods

Materials used: Seeds of wheat (*Triticum aestivum*), barley (*Hordeum vulgare*), chickpea (*Cicer arietinum*) and mungbean (*Vigna radiata*) were used for the experiments. CR, Thioflavin-T, and acid fuchsin were obtained from Sigma Aldrich. Proteostat® aggregation assay kit was obtained from Enzo Life Sciences. Calcofluor white, xylene, ethanol and

neutral buffered formalin (4%) were procured from Thermo Scientific. Leica paraffin wax is used for embedding and Superfrost microscopic slides for histochemical staining were from HiMedia. Leica Microtome was used to obtain all the sections. The sections of all the seeds had a thickness of 8 µm. Visualization was enabled by Leica DM 2500 widefield fluorescent microscope equipped with cross-polarizers and Leica SP5 confocal microscope.

Sectioning of the seeds: The processing was done as per the standard protocols (43, 44) and was optimized to facilitate staining and visualization with different dyes. Briefly, the seeds were washed, surface-sterilized, cut in half using scalpels and incubated in 4% neutral buffered formalin at room temperature for 2 hours. The samples were then transferred to 4˚C for overnight fixation. After washing the fixed seeds 2-3 times with phosphate buffered saline solution, the samples were dehydrated with successive gradients of ethanol (30%, 50%, 70%, 90%), with each ethanol gradient treatment for 30 minutes. Gradient dehydration was followed by treatment of the samples with 100% ethanol twice, for 1 hour each. The samples were then permeated with xylene followed by a mixture of xylene and paraffin in the ratio of 1:1 for 1 hour. Xylene was discarded and paraffin embedding was continued by incubating overnight at 60˚C. The samples were then transferred to paraffin blocks and stored at 4˚C for further use. From the blocks, 8 µm sections were cut and were carefully transferred to glass slides. The slides were heat-fixed on hot plates for 30 minutes at 60˚C and stored at 4˚C for further use. For germination study, the seeds were imbibed in cotton soaked with water in dark. After imbibition, the same procedure for fixation and processing was done.

Histochemical staining of tissue sections: The processed slides were heated for 2-3 minutes at 70˚C and immediately transferred to xylene for 2 minutes in coplin jars. The slides were treated with successive gradients of ethanol (100%, 95%, and 70%) for 5 minutes each. For 95% and 70% alcohol concentrations, the treatments were repeated once. The slides are then washed with distilled water for 10 minutes.

For **SEM** analysis, after water wash, the slides were air-dried and dehydrated in a vacuum desiccator overnight. The samples were then sputter-coated with gold and visualized by Carl Zeiss Evo 18 SEM (10 kV).

For staining, the slides after water wash were dipped in coplin jars containing the staining solution. Acid fuchsin (0.35%) and Calcofluor white (10% v/v) stain was applied on the slides for 1 minute. Saturated solution of CR was used for amyloid detection by incubating the slides in the staining solution for 20 minutes. Proteostat® dye was reconstituted (75 µL) in

10 ml of 1X assay buffer according to the manufacturer's protocol. For ThT (20 μM) and Proteostat® staining, 10 μL of the dye was added on the tissue sections.

Acid fuchsin stained sections were visualized under bright-field and wide-field fluorescence microscopy using the red emission filter. Calcofluor white was observed using the blue emission filter. Birefringence and CR binding were observed using bright-field microscopy and by rotating the polarisers. Proteostat® was observed using the red emission filter. All these images were collected using Leica DM2500 fluorescent microscope equipped with cross-polarizers. ThT signal of seed sections was visualized by Leica TCS SP5 confocal system using He-Ne 488 laser (at 20% laser power) at 10X and 40X (under oil emersion). For each magnification, 40 z-stacks were collected. Quantification of the ThT signal was performed by measuring the ratio of intensity to area for selected areas of each type of tissue using ImageJ analysis. For this, 5 stacks were considered for each seed section. For germination study, the seed sections were stained with CR and ThT. The birefringence due to CR staining was observed using polariser microscope. ThT signal in this case, was visualized using Leica DM 2500 widefield fluorescence microscope using green emission filter. The intensity for three areas of each section was measured and normalized to area to calculate changes in intensity using ImageJ. The graphs were plotted using Origin Pro 9.1.

For each experimental groups, at least three seeds were sectioned and for each probe, at least three random sections have been chosen to perform the experiments. For statistical tests, one-sampled t-test was used. The bars are plotted as means of the individual data points with error bars signifying the standard error of mean.

Isolation of protoplasts from barley and chickpea: Barley grains were dembryonated and cut into quarter grains. These were incubated in 50 mM arginine and 20 mM calcium chloride for 72 hours. After this time-period, the endosperm was removed from each quarter grain using needles under a dissection microscope. These quarter grains were incubated for 48 hours in protoplast isolation media containing 0.35 M mannitol, 2% glucose, 10 mM arginine, 20 mM calcium chloride and 4.5% cellulase. After 48 hours, the media was discarded and protoplast incubation media containing 0.67 M mannitol, 2% glucose and 10 mM arginine, was added. The protoplasts are freed by gentle swirling and allowed to settle for 4 hours. The protoplasts were stored at -80 degree Centigrade in protoplast incubation media containing 5% DMSO and 10% glycerol. For dicot seeds, 0.5 g seeds were cut into 0.5-1 mm strips using scalpel and transferred immediately to 10 ml enzyme solution

containing 20 mM KCl, 20 mM citrate, 0.5 mM manitol and 1.2% cellulase, 10 mM calcium chloride and 0.1% BSA. The mixture was incubated at room temperature in dark for 6 hours at 30 rpm. The enzyme solution was two-fold diluted with wash solution containing 154 mM sodium chloride, 125 mM calcium chloride, 5 mM KCl and 4 mM citrate. The mixture was allowed to settle down under gravity. The upper layer was discarded carefully and the lower layer was resuspended in 5 ml wash solution and incubated on ice for 30 minutes. The protoplast pellet was resuspended in incubation solution containing 0.4 M mannitol, 15 mM magnesium chloride, 4 mM citrate at pH 5.6. For protoplast treatment with plant hormones, these were treated with 20 µM gibberellic acid, or 20 µM abscisic acid or equimolar mixture of both for 8 hours. The protoplasts were then stained with 20 µM ThT.

Acknowledgements: We are thankful to Prof. Pradip Sinha and Prof. Amitabha Bandyopadhyay for letting us use their confocal imaging facility and ultramicrotome facility. We also thank Mr. Upendra Singh Yadav and Mr. Saurabh Singh Parihar for helping with the facilities. N.S and T.Z. acknowledge University Grants Commission for Senior Research Fellowship.

Author Contributions: The study was conceptualized by A.K.T. The experiments were designed by N.S, A.Y.G and A.K.T. The experiments were performed by N.S., T.Z and A.Y.G. Paper was written by N.S. and A.K.T. Data was analysed by all authors.

Data Availability: There are no restrictions in data availability and the corresponding author can be contacted regarding this.

Code Availability: No algorithms are used.

References:

1. Shewry PR, Halford NG. Cereal seed storage proteins: structures, properties and role in grain utilization. Journal of experimental botany. 2002;53(370):947-58.
2. Shewry PR, Napier JA, Tatham AS. Seed storage proteins: structures and biosynthesis. The Plant cell. 1995;7(7):945-56.
3. Tosi P, Gritsch CS, He J, Shewry PR. Distribution of gluten proteins in bread wheat (Triticum aestivum) grain. Annals of botany. 2011;108(1):23-35.

4. Xiong F, Yu XR, Zhou L, Wang Z, Wang F, Xiong AS. Structural development of aleurone and its function in common wheat. Molecular biology reports. 2013;40(12):6785-92.
5. Buttrose M. Ultrastructure of the Developing Aleurone Cells of Wheat Grain. Australian Journal of Biological Sciences. 1963;16(4):768-74.
6. Nadaud I, Tasleem-Tahir A, Chateigner-Boutin A-L, Chambon C, Viala D, Branlard G. Proteome evolution of wheat (Triticum aestivum L.) aleurone layer at fifteen stages of grain development. Journal of Proteomics. 2015;123:29-41.
7. Reyes FC, Chung T, Holding D, Jung R, Vierstra R, Otegui MS. Delivery of Prolamins to the Protein Storage Vacuole in Maize Aleurone Cells. The Plant Cell. 2011;23(2):769-84.
8. BETHKE PC, SWANSON SJ, HILLMER S, JONES RL. From Storage Compartment to Lytic Organelle: The Metamorphosis of the Aleurone Protein Storage Vacuole. Annals of Botany. 1998;82(4):399-412.
9. Hughes JS, Swanson B. MICROSTRUCTURE OF LENTIL SEEDS (Lens Culinaris). Food Structure. 1986;5:8.
10. Brillouet J-M, Carré B. Composition of cell walls from cotyledons of Pisum sativum, Vicia faba and Glycine max. Phytochemistry. 1983;22(4):841-7.
11. Derbyshire E, Wright DJ, Boulter D. Legumin and vicilin, storage proteins of legume seeds. Phytochemistry. 1976;15(1):3-24.
12. Craig S, Millerd A. Pea seed storage proteins — Immunocytochemical localization with protein a-gold by electron microscopy. Protoplasma. 1981;105(3):333-9.
13. Abirached-Darmency M, Dessaint F, Benlicha E, Schneider C. Biogenesis of protein bodies during vicilin accumulation in Medicago truncatula immature seeds. BMC Research Notes. 2012;5(1):409.
14. Herman E, Schmidt M. Endoplasmic Reticulum to Vacuole Trafficking of Endoplasmic Reticulum Bodies Provides an Alternate Pathway for Protein Transfer to the Vacuole. Plant Physiology. 2004;136(3):3440-6.
15. Schmidt SR. Protein Bodies in Nature and Biotechnology. Molecular Biotechnology. 2013;54(2):257-68.
16. Narayanaswamy R, Levy M, Tsechansky M, Stovall GM, O'Connell JD, Mirrielees J, et al. Widespread reorganization of metabolic enzymes into reversible assemblies upon nutrient starvation. Proceedings of the National Academy of Sciences. 2009;106(25):10147-52.
17. Peters LZ, Karmon O, David-Kadoch G, Hazan R, Yu T, Glickman MH, et al. The Protein Quality Control Machinery Regulates Its Misassembled Proteasome Subunits. PLOS Genetics. 2015;11(4):e1005178.
18. Pezza JA, Villali J, Sindi SS, Serio TR. Amyloid-associated activity contributes to the severity and toxicity of a prion phenotype. Nature Communications. 2014;5(1):4384.
19. Chiti F, Dobson CM. Protein Misfolding, Functional Amyloid, and Human Disease. Annual Review of Biochemistry. 2006;75(1):333-66.
20. Dobson CM. The Amyloid Phenomenon and Its Links with Human Disease. Cold Spring Harbor perspectives in biology. 2017;9(6):a023648.
21. Antonets KS, Nizhnikov AA. Amyloids and prions in plants: Facts and perspectives. Prion. 2017;11(5):300-12.
22. Antonets KS, Belousov MV, Sulatskaya AI, Belousova ME, Kosolapova AO, Sulatsky MI, et al. Accumulation of storage proteins in plant seeds is mediated by amyloid formation. PLoS Biol. 2020;18(7):e3000564.
23. Kumar R, Singh R, Misra JP, Yadav A, Kumar A, Yadav R, et al. Dissecting Proteomic Estimates for Enhanced Bioavailable Nutrition during Varied Stages of Germination and Identification of Potential Genotypes in Chickpea. LEGUME RESEARCH - AN INTERNATIONAL JOURNAL. 2021.
24. Uppal V, Bains K. Effect of germination periods and hydrothermal treatments on in vitro protein and starch digestibility of germinated legumes. J Food Sci Technol. 2012;49(2):184-91.

25. Zhao M, Zhang H, Yan H, Qiu L, Baskin CC. Mobilization and Role of Starch, Protein, and Fat Reserves during Seed Germination of Six Wild Grassland Species. Frontiers in Plant Science. 2018;9(234).
26. Bønsager BC, Finnie C, Roepstorff P, Svensson B. Spatio-temporal changes in germination and radical elongation of barley seeds tracked by proteome analysis of dissected embryo, aleurone layer, and endosperm tissues. Proteomics. 2007;7(24):4528-40.
27. Shen D, Coleman J, Chan E, Nicholson TP, Dai L, Sheppard PW, et al. Novel cell- and tissue-based assays for detecting misfolded and aggregated protein accumulation within aggresomes and inclusion bodies. Cell Biochem Biophys. 2011;60(3):173-85.
28. Benson MD, Buxbaum JN, Eisenberg DS, Merlini G, Saraiva MJM, Sekijima Y, et al. Amyloid nomenclature 2020: update and recommendations by the International Society of Amyloidosis (ISA) nomenclature committee. Amyloid : the international journal of experimental and clinical investigation : the official journal of the International Society of Amyloidosis. 2020;27(4):217-22.
29. Nielsen LF, Moe D, Kirkeby S, Garbarsch C. Sirius red and acid fuchsin staining mechanisms. Biotechnic & histochemistry : official publication of the Biological Stain Commission. 1998;73(2):71-7.
30. Herrera-Ubaldo H, de Folter S. Exploring Cell Wall Composition and Modifications During the Development of the Gynoecium Medial Domain in Arabidopsis. Frontiers in Plant Science. 2018;9(454).
31. Boke E, Ruer M, Wühr M, Coughlin M, Lemaitre R, Gygi SP, et al. Amyloid-like Self-Assembly of a Cellular Compartment. Cell. 2016;166(3):637-50.
32. Naiki H, Gejyo F. [20] Kinetic analysis of amyloid fibril formation. Methods in Enzymology. 309: Academic Press; 1999. p. 305-18.
33. Navarro S, Ventura S. Fluorescent dye ProteoStat to detect and discriminate intracellular amyloid-like aggregates in Escherichia coli. Biotechnology Journal. 2014;9(10):1259-66.
34. Oshinbolu S, Shah R, Finka G, Molloy M, Uden M, Bracewell DG. Evaluation of fluorescent dyes to measure protein aggregation within mammalian cell culture supernatants. J Chem Technol Biotechnol. 2018;93(3):909-17.
35. Laor D, Sade D, Shaham-Niv S, Zaguri D, Gartner M, Basavalingappa V, et al. Fibril formation and therapeutic targeting of amyloid-like structures in a yeast model of adenine accumulation. Nature Communications. 2019;10(1):62.
36. Murphy CL, Eulitz M, Hrncic R, Sletten K, Westermark P, Williams T, et al. Chemical typing of amyloid protein contained in formalin-fixed paraffin-embedded biopsy specimens. American journal of clinical pathology. 2001;116(1):135-42.
37. Bleem A, Daggett V. Structural and functional diversity among amyloid proteins: Agents of disease, building blocks of biology, and implications for molecular engineering. Biotechnology and Bioengineering. 2017;114(1):7-20.
38. Kumar V, Sinha N, Thakur AK. Necessity of regulatory guidelines for the development of amyloid based biomaterials. Biomaterials science. 2021;9(12):4410-22.
39. Matiiv AB, Trubitsina NP, Matveenko AG, Barbitoff YA, Zhouravleva GA, Bondarev SA. Amyloid and Amyloid-Like Aggregates: Diversity and the Term Crisis. Biochemistry (Moscow). 2020;85(9):1011-34.
40. Wetzel R. Exploding the Repeat Length Paradigm while Exploring Amyloid Toxicity in Huntington's Disease. Accounts of Chemical Research. 2020;53(10):2347-57.
41. Santos J, Ventura S. Functional Amyloids Germinate in Plants. Trends in Plant Science. 2021;26(1):7-10.
42. Maury CPJ. Amyloid and the origin of life: self-replicating catalytic amyloids as prebiotic informational and protometabolic entities. Cellular and Molecular Life Sciences. 2018;75(9):1499-507.

43. Jääskeläinen A-S, Holopainen-Mantila U, Tamminen T, Vuorinen T. Endosperm and aleurone cell structure in barley and wheat as studied by optical and Raman microscopy. Journal of Cereal Science. 2013;57(3):543-50.
44. Wood JA, Knights EJ, Choct M. Morphology of Chickpea Seeds (Cicer arietinum L.): Comparison of desi and kabuli Types. International Journal of Plant Sciences. 2011;172(5):632-43.